Cloud evaluation using satellite observations

F. Chevallier, P. Bauer, G. Kelly, A. P. McNally, C. Jakob

European Centre for Medium-Range Weather Forecasts

Summary: Infrared and Micro-wave measurements from Vertical Temperature Profile Radiometer (VTPR), High-resolution Infrared Radiation Sounder (HIRS) and Microwave Sounding Unit observations (MSU) on-board the National Oceanic and Atmospheric Administration (NOAA) satellites have been providing information about cloud system shape and intensity on global scale since 1972. Such radiation observations are a key element in the evaluation of ERA-40, so cloud-affected radiances from the model as from the observations are part of the archive. Furthermore, cloud variables derived from the observations are a product of the re-analysis of direct climatological relevance.

In the present study, NOAA-11 HIRS/2 and MSU measurements are used to assess the characteristics of the cloud fields produced by the ERA-40 forecasting system over mid-latitude and tropical oceans. Infrared and micro-wave radiation have different sensitivities to clouds and are therefore complementary. Observed and model-generated radiances, as well as HIRS/2-derived cloud parameters, are compared.

The model clouds are shown to be well distributed, with realistic seasonal cycles. However, deficiencies are identified and discussed: the radiative impact of both high clouds and stratocumulus is too low, the frequency of occurrence of low clouds is overestimated, the frequency of occurrence of high clouds is overestimated in the Inter-Tropical Convergence Zone.

1 Introduction

Clouds have a high variability in time and space. As large reservoirs of latent heat, they exert a major influence on the atmospheric energy balance. Also the atmospheric heating rates are strongly affected by the interaction of clouds with visible and infrared electro-magnetic waves. However, through emission, absorption, reflection and scattering processes, this interaction itself makes it difficult to observe clouds from a distance. For satellite measurements, complex algorithms are used either to retrieve the cloud information (e.g., Rossow and Schiffer 1991; Wylie *et al.* 1994; Stubenrauch *et al.* 1999; Baum *et al.* 2000) or to remove it in order to get cloud-clear products (e.g., McMillin and Dean 1982; Munro *et al.* 2000).

Cloud-affected narrow-band and broad-band spectral satellite measurements, as well as derived cloud variables, form valuable data-sets for atmospheric studies. They have also become an essential part of the validation of atmospheric general circulation models (Le Treut and Li 1988; Morcrette 1991a; Shah and Rind 1995; Bony *et al.* 1997). As such, the observations from the VTPR and TIROS-N Operational Vertical Sounder (TOVS) instruments on-board the NOAA polar-orbiting satellites are an important part of the evaluation of the analysis/forecast system at ECMWF, in particular for ERA-40.

In this paper, the 6-hour forecast from ERA-40 is compared to the HIRS/2 and MSU data from the TOVS over mid-latitude and tropical oceans (60°S-60°N). The data and the model are described in section 2. Model-equivalent infrared and micro-wave radiances are computed from the model variables using a forward radiation scheme detailed in section 3. For MSU, the model-observation comparison is made for the radiances only. The cloud variables retrieved from HIRS with the CO_2-slicing technique described by Wylie *et al.* (1994) are useful for comparisons with the model. They implicitly contain part of the multi-spectral information of the radiometer. However these cloud variables are to be understood as *radiatively effective* quantities, in the sense that they are defined as seen from the

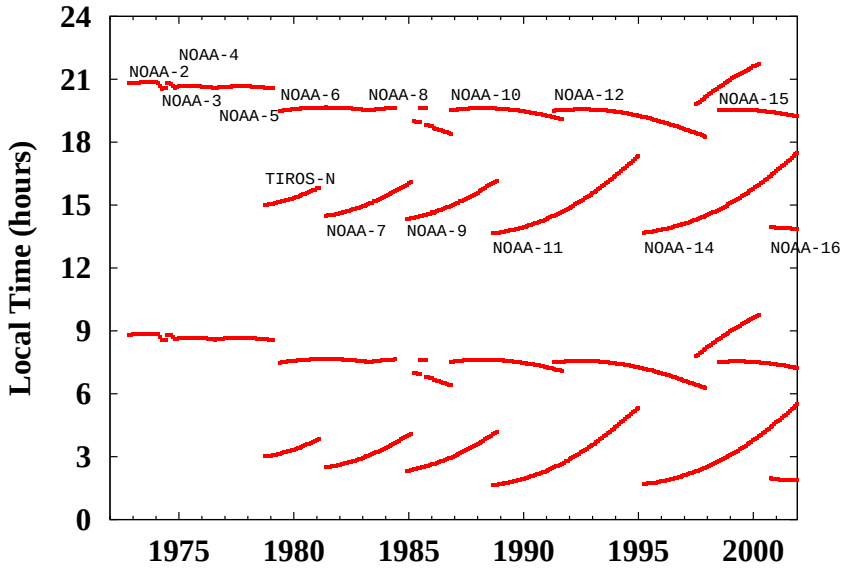

Figure 1: Local Solar Time (LST) at the equator for the NOAA and TIROS-N satellites. Times before (after) 12 correspond to descending (ascending) node. NOAA-2 to -5 satellites carry VTPR, TIROS-N and NOAA-6 to -14 platforms carry TOVS, ATOVS is onboard NOAA-15 and -16.

satellite. Therefore in the present study, the CO_2-slicing technique of Wylie *et al.* (1994, 1999) is used to derive cloud top pressure and effective cloud emissivity from the observed HIRS brightness temperatures as well as from the model-derived ones. The method is detailed in section 3. The MSU radiance comparison is presented in section 4. The HIRS radiance and the HIRS-derived cloud variable comparisons are shown in section 5. The conclusions are outlined in section 6.

2 The data

2.1 The TOVS data

The MSU radiometer of TOVS comprises four channels for making passive measurements in the 5.5 millimetre wavelength oxygen region. Their weighting functions respectively peak at the surface, at 700hPa, at 300hPa and at 90hPa. An MSU spot has a typical circular shape of 54.7 km radius at nadir and an elliptic shape of axis 323.1 and 178.8 km at the end of the scan (Kidwell 1998).

The HIRS/2 instrument of TOVS measures radiation in 20 channels covering both the long-wave and the short-wave parts of the spectrum. The ground instantaneous field of view is typically a circle of 17.4 km diameter at nadir. At the end of the scan, the ground field of view is 58.5 km cross-track by 29.9 km along-track (Kidwell 1998).

As an illustration of the use of TOVS data in ERA-40 for cloud evaluation, the raw radiances for HIRS and MSU are taken here from the NOAA-11 satellite during January and July 1990. NOAA-11 operates in a near-polar, sun-synchronous orbit, with about 14 orbits per day. As reported in Figure 1, its ascending orbits cross the equator at about 14 LST. Due to the high volume of data, only one HIRS spot over four is processed here, irrespective of scan angle. All MSU spots are used.

Various biases affect the brightness temperatures throughout the life of an instrument. The data used here are bias-corrected with the ECMWF operational method described by Harris and Kelly (2001). The computed biases can reach several degrees K in some channels. In the framework of the CO_2-slicing method described below, these corrections were shown to improve the consistency between the

different channels.

2.2 The model fields

The model data come from the experiment 0018 of ERA-40. The final version of the re-analysis will differ only by minor improvements from the system used in that run for the period considered.

In the following, 6-hour forecasts at 00, 06, 12 and 18 UTC are compared to the TOVS data in the 6-hour window that is centred around the forecast time. Model data are interpolated at observation points and at observation times. As the resolution of the model (about 125 km from the equator to the poles) and that of the observations differ, emphasis is put here on monthly statistics rather than on instantaneous comparisons.

3 Comparing model and satellite data

3.1 Radiation model

The present study uses a modified version of the Radiative Transfer for Tiros Operational Vertical Sounder (RTTOV: Eyre, 1991; Saunders *et al.*, 1999) scheme that takes cloud absorption into account in a way similar to the ECMWF operational broad-band infrared radiation scheme (Morcrette 1991b). Similar work was done for HIRS/2 on a previous version of the ECMWF system but was never used routinely (Rizzi 1994).

Following the multi-layer grey body approach (Washington and Williamson 1977), clouds are introduced as grey bodies. Their contribution to the radiances is determined by their horizontal coverage n^i and their emissivity ϵ_ν^i in each vertical layer i of the model. ϵ_ν^i is derived from the cloud liquid (and/or ice) water path l^i by the following equation:

$$\epsilon_\nu^i = 1 - e^{-k_\nu^i l^i} \tag{1}$$

where k_ν^i is the extinction coefficient at frequency ν. Its value varies according to the nature (liquid or ice) of the cloud, the assumed particle size spectra and particle temperature.

This approach enables the radiances in the presence of semi-transparent cloud layers to be expressed as a linear combination of the clear sky radiance L_ν^{Clr}, and of the radiances in the presence of single layered clouds treated as black bodies, L_ν^i. The coefficients of the linear combination are functions of the n^is and of the ϵ_ν^is and depend on the way the cloudy layers overlap. Surface reflection of the cloud downward emission is taken into account because it has a strong impact over sea for micro-waves.

Various overlapping hypotheses can be used according to the vertical structure of the clouds (Morcrette and Jakob 2000). The maximum-random hypothesis, as described by Räisänen (1998) is used here. It explicitly distinguishes between the horizontal coverage and the emissivity of the cloud layers, as is done in the current operational broad-band scheme.

Cloud absorption is taken into account in the infrared spectrum following Ebert and Curry (1992) for ice water and Smith and Shi (1992) for liquid water. The single scattering albedo is usually small for the infrared wavelengths above 5 μm at the top of the atmosphere and is neglected. Consistently with the broadband radiation model, ice particle radii vary between 30 and 60 μm with a temperature dependency from Ou and Liou (1995). Liquid particle radius is set to 10 μm over land and 13 μm over sea.

Cloud absorption is introduced in the microwave spectrum in the range from 1-200 GHz as a direct function of frequency and liquid water/ice content. Comparison to full Mie-calculations using modified Gamma-distributions adjusted to water contents for particle size indicated that: (1) scattering by droplets can be neglected for all currently used microwave channels (i.e. the single scattering albedo is less than 0.002) while scattering by ice particles may become significant for $\nu > 60$ GHz (i.e. the single scattering albedo may be more than 0.01); (2) the shape of droplet size spectra is negligible. Ice and water dielectric properties were calculated following Hufford (1991) and Liebe *et al.* (1989), respectively. Rain-radiation interaction in the microwave is important but is not considered here since its scattering properties do not fit within the multi-layer grey body framework. More elaborated, and therefore more computationally-expensive, parameterisations are needed.

3.2 Strategy for the MSU comparison

Estimating the micro-wave land surface emissivity is difficult (Prigent *et al.* 1997). Over open sea, the lower values of the emissivities (around 0.5) as well as their smaller horizontal variability makes the extraction of information from the micro-wave data easier. As a consequence, the present study with MSU is restricted to ocean data between 60°S and 60°N only. The Ulaby *et al.* (1981) model provides the sea emissivity.

Among the four MSU channels, the three atmosphere-sounding ones (channels 2 to 4) are not significantly affected by clouds (except channel 2 for deep water clouds). Indeed ice water has negligible impact on the radiances around 50 GHz. Therefore results are presented here for the window channel (channel 1) as the difference between the cloud-affected radiance (either from the model or from the observation) and the clear-sky radiance from the model. In the case of a perfect model, this difference is a function of liquid water and rain profiles only. In fact, uncertainties in the surface temperature and the water vapour profile degrade the accuracy of the model clear-sky radiances. But the largest signal is due to clouds.

3.3 Strategy for the HIRS comparison

Understanding radiance variations in 19 channels is an evolving study. Moreover, the useful information from HIRS is contained not only in the channel brightness temperatures themselves, but also in their relative values with respect to each other.

Among the 20 channels, the present study makes use of four of them (channels 4 to 7) that are located in the CO_2 band around $14\mu m$, and of one (channel 8) that is located in the $11\mu m$ so-called "window" region. Following the work of Smith and Platt (1978), the CO_2-slicing method is used to retrieve cloud variables from these five channels. The retrieved quantities are the cloud top pressure P_i and the effective cloud amount $(n\epsilon)_\nu$ defined as:

$$L_\nu(\theta) = (n\epsilon)_\nu L^i_\nu(\theta) + [1 - (n\epsilon)_\nu] L^{Clr}_\nu(\theta) \tag{2}$$

where L^i_ν is the top-of-the-atmosphere up-welling radiance emitted at frequency ν by a black-body placed at pressure level P_i.

Assuming that $(n\epsilon)_\nu$ is the same for two adjacent frequencies, equation (2) allows for successive estimations of P_i and of $(n\epsilon)_\nu$. L^i_ν and L^{Clr}_ν are computed here from a previous run of RTTOV from model temperature, absorbing gas profiles and surface characteristics. Four pairs of channels are used from channels 4 to 7 of HIRS. The final variables are those that satisfy the radiative transfer the best. $(n\epsilon)_\nu$ is provided for the 11 μm HIRS channel. As described in Wylie *et al.* (1994), a series of quality checks are performed. If the solution is rejected, a rough estimation is performed using equation (2)

with $(n\epsilon)_\nu = 1.0$ in the 11 μm window channel. Retrieved cloud layers below 700 hPa (about 3 km) are most likely to correspond to this simple estimation because the CO_2-slicing method is not capable of retrieving $(n\epsilon)_\nu$ in the lower troposphere.

The sources of error of the method are discussed in Menzel *et al.* (1992). Over open seas, the main issue appears to be multi-layer cloud situations where the algorithm can only retrieve a single layer that may be below the highest transmissive cloud, depending on the emissivity of the clouds below. Due to reduced sensitivity of the infrared sounder in the lower troposphere, as well as to possible temperature inversions close to the surface, the method is not accurate for low clouds.

The CO_2-slicing technique is applied after a rough cloud detection test based on a threshold on channel 8: a cloud is diagnosed when the observed radiance in the 11 μm channel is lower than the model clear sky radiance in the same channel by more than 1 $mW.m^{-2}.sr^{-1}.cm^{-1}$. This cloud detection strongly relies on the quality of the surface temperature estimation. As a consequence, the present study with HIRS is also restricted to ocean data between 60°S and 60°N only, because sea-surface temperature is estimated very accurately from infrared and visible channels observations. It has also a much weaker diurnal cycle than land surface temperature. The sea surface temperature fields come from 5-day averages of updated National Center for Environmental Prediction (NCEP) analyses. A functional fit to the tables provided by Masuda *et al.* (1988) provides the infrared sea emissivity (T. J. Kleespies, personal communication).

4 MSU comparison

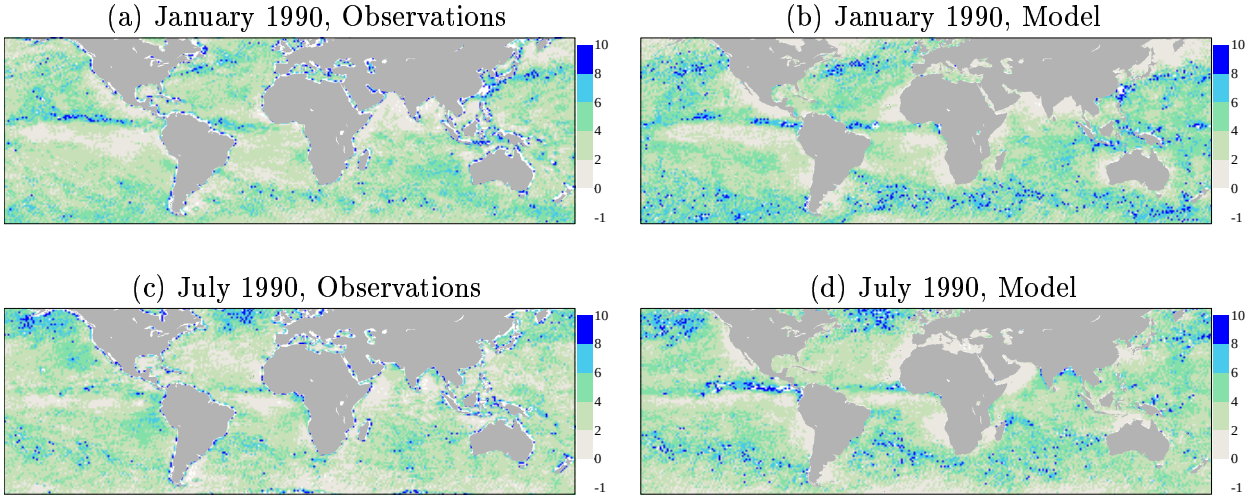

Figure 2: Observed and simulated MSU channel 1 minus model clear-sky MSU channel 1. NOAA-11 descending orbits.

The mean value of the difference between the cloud-affected MSU-1 brightness temperature and the model clear-sky MSU-1 brightness temperature is presented in Figure 2 for the two months. For the model, the differences are always positive because clouds are seen as warm bodies over the low-emitting sea surface. For the observations, small negative values may occur due to inaccurate sea surface temperature and emissivity. Despite the limitations due to neglecting precipitation absorption and scattering in the simulated radiances, a good qualitative agreement is found in the shape of the ascending-motion regions, like the Inter-Tropical Convergence Zone (ITCZ), the South-Pacific Convergence Zone (SPCZ) and the storm tracks. In the descending-motion regions, the model values are significantly lower than the observation ones. In particular, in the stratocumulus regions off the West

coast of the continents, the simulated micro-wave radiances are hardly affected by clouds. This may indicate that the model underestimates liquid water in these regions. However, an underestimation of the surface temperature and/or emissivity there would yield the same result. The study of the infrared radiances brings more information about this matter.

5 HIRS/2 comparison

5.1 HIRS $11\mu m$ brightness temperature

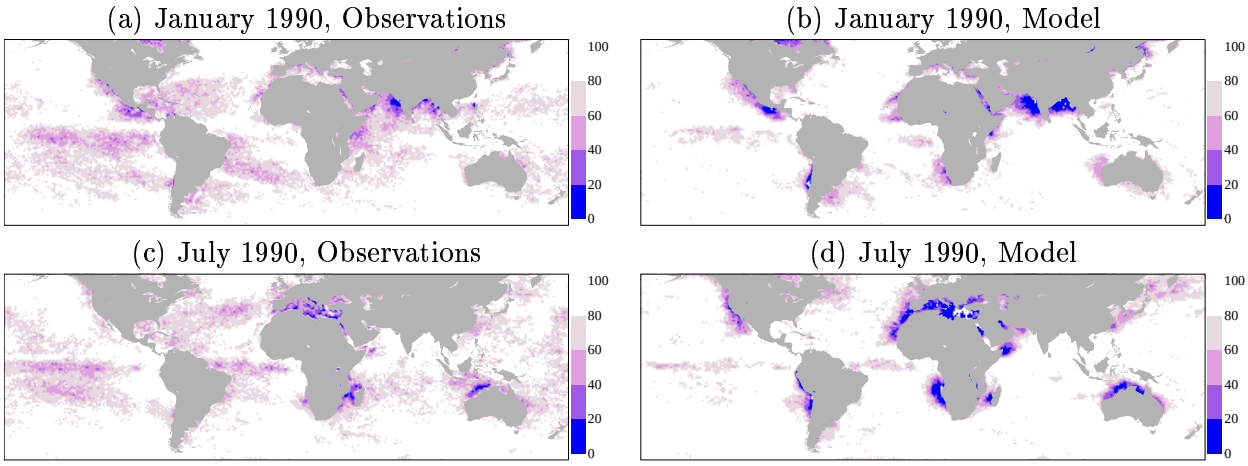

Figure 3: Frequency of cloud over the oceans in the observations (left column) and in the model (right column). NOAA-11 descending orbits.

As detailed in section 3.4, a cloud detection based on a threshold test on the $11\mu m$ channel is used here. Figure 3 presents the frequencies of occurrence of estimated cloud-free points. With this diagnosis, the model appears to have more clouds than the observations in most regions of the globe, except in the stratocumulus regions off the West coast of the continent in both seasons, and around Northern Africa in the boreal summer season only. A lack of cloudiness in these regions is consistent with the micro-wave results presented in section 4. The differences in the other regions are discussed in section 6.

5.2 Retrieved cloud type

A simple three-category cloud classification is defined for the clouds, based on the CO_2-retrieved cloud top: high-top (cloud top above 400 hPa), middle-top (cloud top between 400 and 700 hPa), and low-top (cloud top below 700 hPa). The CO_2-slicing method is particularly reliable for the high-top cloud category (Jin *et al.* 1996). The occurrence frequency of each cloud type is shown in Figure 4 (boreal winter season) and Figure 5 (boreal summer season).

There is a good qualitative agreement between the model and the observation for the ITCZ structure: the seasonal variations of the narrow-banded high-top cloud structure are comparable in both, as well as its broadening in the Pacific and Indian oceans due to large warm-ocean pools, Indonesian low and summer monsoon flows (e.g. Waliser and Gautier 1993). The model appears to produce higher frequencies of cirrus clouds in the Atlantic and the East Pacific ITCZ, where the model occurrence is about 70% in boreal summer instead of about 50% for the observations. The South-Pacific Convergence Zone (SPCZ) is created by convergence of the South-East trade winds in the Pacific and mainly

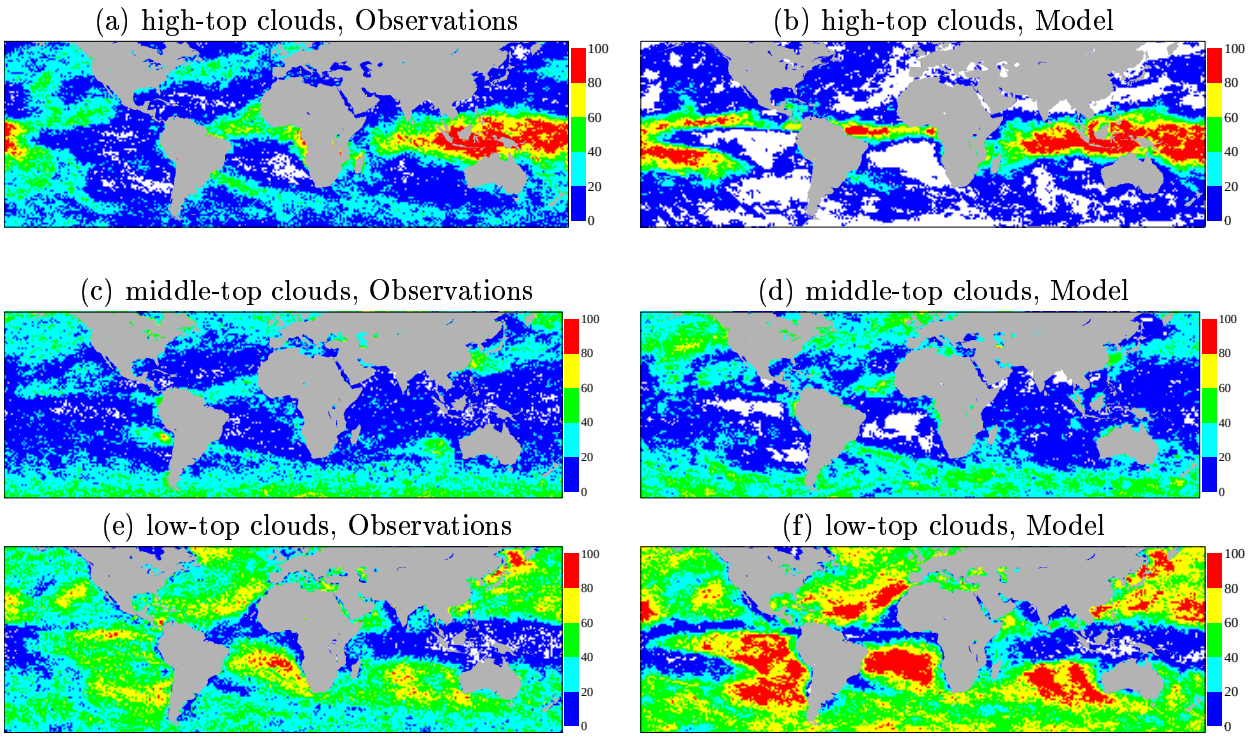

Figure 4: Occurrence frequency of high-, middle- and low-top clouds for January 1990 over the oceans in the observations (left column) and in the model (right column). NOAA-11 descending orbits.

develops in the austral summer season. It is reasonably well reproduced by the model. Similarly, the austral summer South Atlantic Convergence Zone (SACZ) and South Indian Convergence Zone (SICZ) as defined by Cook (2000) can be identified in the model, but the frequencies of clouds in each category are different from those in the observations.

The stratus clouds off the west coast of the subtropical continents are usually associated with atmospheric subsidence over cold sea surface temperature with sharp temperature inversions in the boundary layer (e.g. Klein and Hartmann 1993). These regions are mainly cloud free in the model (Figure 5), even though the stratus clouds are known to be dense and numerous. Surprisingly, off the Peruvian coast and California, the observations report middle-top clouds. It is likely that temperature inversions and low vertical gradients induce higher cloud-tops than in reality with the CO_2-slicing technique. In any case, the model poorly represents the clouds in these regions.

As the westward trade winds come closer to the ITCZ, where the sea surface is warmer, cumulus becomes the dominant cloud type (e.g. Klein and Hartmann 1993). From the observed infrared radiances, large occurrences of low clouds are depicted. The occurrences of low clouds as seen from the model radiances are even higher (about 90%).

The storm tracks in both hemispheres have a high variability in both space and time. They appear in all three cloud categories in the observations. The model storm tracks have less high clouds.

As a complementary study (not shown), the main tropical and extra-tropical cyclones have been individually examined. No systematic deficiency could be identified for the mid-latitude fronts, other than the above-mentioned misrepresentation of high clouds, whereas Jakob and Rizzi (1997) described the fronts as too narrow in a previous version of the model. On the other hand, tropical cyclones appear to be too spread.

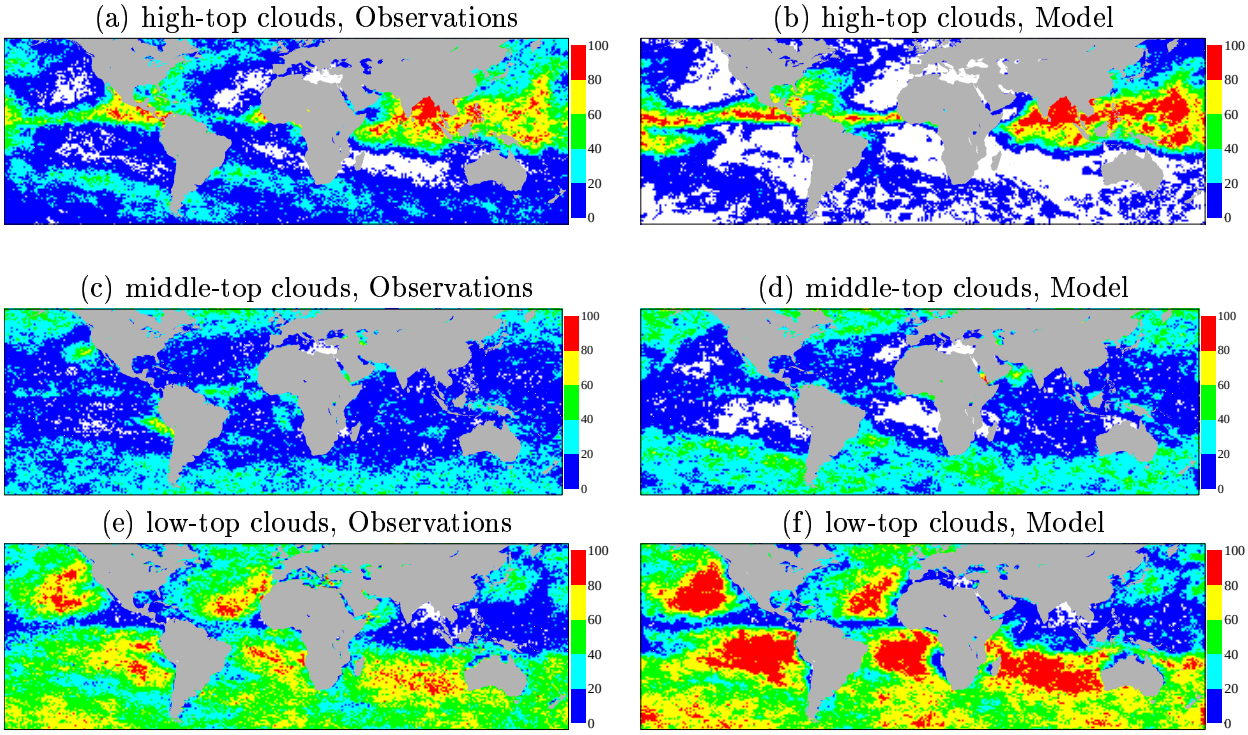

Figure 5: Occurrence frequency of high-, middle- and low-top clouds for July 1990 over the oceans in the observations (left column) and in the model (right column). NOAA-11 descending orbits.

6 Discussion

In the previous sections cloudy radiances in two spectral regions and derived cloud information as observed by the TOVS instruments were compared with those simulated using short-range forecasts from the ECMWF model in the configuration used for the ERA-40 project. Further results are documented by Chevallier *et al.* (2002). This study aimed at identifying deficiencies in the representation of clouds in the ECMWF model, even though the use of the sole top-of-the-atmosphere radiation does not necessarily give a full insight into the characteristics of the model clouds. In summary of the previous sections the following features in the model have been identified.

- too little cloud-radiative effects of stratocumulus, apparent both at micro-wave and infrared wavelengths
- an overestimation of cloud top pressure (as derived by CO2-slicing) in mid-latitudes
- an overestimation of the frequency of occurrence of low clouds except in the stratocumulus regions
- on overestimation of the frequency of occurrence of high clouds in the ITCZ
- a strong underestimation of the frequency of clear sky situations, when they are defined with a simple threshold test

Infrared brightness temperature are affected by many cloud parameters, such as cloud fraction, cloud condensate content, cloud top temperature, particle size and overlap. It is therefore difficult to assign the shortcomings in the radiative properties or derived quantities, such as cloud top pressure, to

individual cloud parameters. However previous studies (Klein and Jakob 1999, Chevallier *et al.* 2002) indicate that a lack of cloud ice or its radiative effects, rather than an underestimation of cloud fraction, is likely to cause the overestimation of effective cloud top pressure in mid-latitudes.

High clouds when present produce too high infrared brightness temperatures. However, their frequency of occurrence is overestimated by the model in the ITCZ. Hence, the lack of radiative effect of high clouds apparent in instantaneous point to point comparisons is over-compensated by predicting their occurrence too frequently, leading to an overestimation of the long-wave effect of the ITCZ in longer-term averages.

The poor representation of stratocumulus clouds and their radiative effects found here is consistent with previous findings by Jakob (1999), Chevallier and Morcrette (2000), and Duynkerke and Teixeira (2001). It should be noted that although the recent increase of the vertical resolution of the ECMWF model from 31 to 60 model levels has slightly improved the simulation of this cloud type (Teixeira, 1999), the model errors remain large. The correct simulation of stratocumulus by GCMs has been identified as a major problem area and work is underway not only at ECMWF to improve their representation.

Another problem identified is the apparent underestimation of the occurrence of clear sky situations in the model (mostly replaced by low-cloud situations). Care has to be taken interpreting that result. It is evident in Figures 4 and 5, that the largest regions with significant occurrence differences are those which usually exhibit low cloud covers such as the cumulus dominated trade wind regions. Typical values of cloud cover in both climatologies and model are on the order of 30 % and individual clouds are at most a few kilometres in horizontal extent. As the model resolution (about 60 km) is lower than the satellite one (about 20 km close to nadir), higher cloud frequencies are expected in the model.

As illustrated here, while not assimilated, cloudy-affected VTPR and TOVS data are a key element of the monitoring of the ECMWF 40-year re-analysis. As a consequence, the model radiances and the CO_2-derived cloud variables from the model and from the VTPR/ HIRS observations are part of the archive. The cloud variables derived from the observations is a product of the re-analysis of direct climatological relevance. VTPR data have never been used before for cloud retrieval with the CO_2-sclicing and the quality of those data will be examined and documented.

Acknowledgements

D. P. Wylie and P. Menzel provided the initial version of the CO_2 slicing subroutine. The authors are grateful to J.-J. Morcrette for fruitful discussions about the cloud absorption parameterisation. The help of E. Andersson and S. Saarinen in introducing the cloud-affected radiance computation in the ECMWF forecast system was greatly appreciated. This work was done at the Satellite Application Facility on Numerical Weather prediction which is co-sponsored by Eumetsat. J.-F. Mahfouf, A. Simmons and D. Wylie helped to improve the initial manuscript.

References

Baum, B. A., P. F. Soulen, K. I. Strabala, M. D. King, S. A. Ackerman, W. P. Menzel, and P. Yang, 2000: Remote sensing of cloud properties using MODIS airborne simulator imagery during SUCCESS. 2. Cloud thermodynamic phase. *J. Geophys. Res.*, **105**, 11781-11792.

Bony, S., Y. Sud, K. M. Lau, J. Susskind, S. Saha, 1997: Comparison and satellite assessment of NASA/DAO and NCEP-NCAR reanalyses over tropical ocean: atmospheric hydrology and radiation. *J. Climate*, **10**, 1441-1462.

Chevallier, F., and J.-J. Morcrette, 2000: Comparison of model fluxes with surface and top-of-the-atmosphere observations. *Mon. Wea. Rev.*, **128**, 3839-3852.

Chevallier, F., P. Bauer, G. Kelly, C. Jakob, and T. McNally, 2002: Model clouds over oceans as seen from space: comparison with HIRS/2 and MSU radiances. *J. Climate*, **14**, 4216-4229.

Cook, K. H., 2000: The South Indian Convergance Zone and interannual rainfall variability over Southern Africa. *J. Climate*, **13**, 3789-3804.

Duynkerke, P. G., and J. Teixeira, 2001: A comparison of the ECMWF re-analysis with FIRE I obsevrations: diurnal variation of marine stratocumulus. *J. Clim.*, **14**, 1466-1478.

Ebert, E. E. and J. A. Curry, 1992 : A parameterization of ice optical properties for climate models. *J. Geophys. Res.*, **97D**, 3831-3836.

Eyre, J. R., 1991: A fast radiative transfer model for satellite sounding systems. *ECMWF Technical Memorandum No. 186.*

Harris, B. A., and G. Kelly, 2001: A Satellite Radiance Bias Correction Scheme for Radiance Assimiliation. *Q. J. Roy. Meteor. Soc.*, **127**, 1453-1468.

Hufford, G., 1991: A model for the complex permittivity of ice. *Int. J. Infrared Millimeter Waves*, **12**, 677-681.

Jakob, C., 1999: Cloud cover in the ECMWF reanalysis. *J. Climate*, **12**, 947-959.

Jakob, C., and R. Rizzi, 1996: Evaluation of model OLR in cloudy regions using TOVS-1B data. *Proc. of the Int. TOVS Study Conference, Igls, Austria, 20-26 February 1997*, 197-206.

Jin, Y, W. B. Rossow, and D. P. Wylie, 1996: Comparison of the climatologies of high-level clouds from HIRS and ISCCP. *J. Climate*, **9**, 2850-2879.

Klein, S. A., and D. L. Hartmann, 1993: The seasonal cycle of low stratiform clouds. *J. Climate*, **6**, 1587-1606.

Klein, S. A., and C. Jakob, 1999: Validation and sensitivities of frontal clouds simulated by the ECMWF model. *Mon. Wea. Rev.*, **127**, 2514-2531.

Kidwell, K. B., 1998: NOAA polar orbiter user's guide. Technical report, U. S. Dept of Commerce/

NOAA/ NESDIS.

Le Treut, H., and Z. Li, 1988: Using Meteosat data to validate a prognostic cloud generation model. *Atmos. res.*, **21**, 273-292.

Liebe, H. J., T. Manabe, and G. A. Hufford, 1989: Millimeter wave attenuation and delay rates due to fog/ cloud conditions. *IEEE Trans. Antennas Propag.*, **37**, 1617-1623.

Masuda, K., T. Takashima, and Y. Takayama, 1988: Emissivity of Pure and Sea Waters for the Model Sea Surface in the Infrared Window Regions. *Remote Sensing of the Environment*, **24**, 313-329.

McMillin, L. M., and C. Dean, 1982: Evaluation of a new operational technique for producing clear radiance. *J. Appl. Meteor.*, **21**, 1005-1014.

Menzel, W. P., D. P. Wylie, and K. I. Strabala, 1992: Seasonal and diurnal changes in cirrus clouds as seen in four years of observations with the VAS. *J. Appl. Meteor.*, **31**, 370-385.

Morcrette, J.-J., 1991a: Evaluation of model-generated cloudiness: satellite observed and model-generated diurnal variability and brightness temperature. *Mon. Wea. Rev.*, **119**, 1205-1224.

Morcrette, J.-J., 1991b: Radiation and Cloud Radiative Properties in the European Centre for Medium Range Weather Forecasts forecasting system. *J. Geophys. Res.*, **96:D5**, 121-9132.

Morcrette, J.-J., and C. Jakob, 2000: The response of the ECMWF model to changes in cloud overlap assumption. *Mon. Wea. Rev.*, **128**, 1707-1732.

Munro, R., G. Kelly, and R. Saunders, 2000: Assimilation of Meteosat Radiance Data within the 4DVAR System at ECMWF. EUMETSAT/ECMWF Fellowship Programme Report.

Ou and Liou, 1995: *Atmos. Res.*, **35**, 127-138.

Prigent, C., W. B. Rossow, and E. Matthews, 1997: Microwave land surface emissivities estimated from SSM/I observations. *J. Geophys. Res.*, **102:18**, 21867-21890.

Räisänen, P., 1998: Effective longwave cloud fraction and maximum-random overlap clouds - a problem and a solution. *Mon. Wea. Rev.*, **126**, 3336-3340.

Rizzi, 1994: Raw HIRS/2 radiances and model simulations in the presence of clouds. ECMWF Technical Memorandum No. 73 [available from ECMWF, Shinfield Park, Reading, Berks. RG2 9AX, UK].

Rossow, W. B., and R. A. Schiffer, 1983: The International Satellite Cloud Climatology Project (ISCCP): the first project of the World Climate Research Program. *Bull. Amer. Meteo. Soc.*, **64**,

779-784.

Saunders, R., M. Matricardi, and P. Brunel, 1999: An improved fast radiative transfer model for assimilation of satellite radiance observations. *Quart. J. Roy. Meteor. Soc.*, **125**, 1407-1425.

Shah, K. P., and D. Rind, 1995: Use of microwave brightness temperatures with a general circulation model. *J. Geophys. Res.*, **100:D7**, 13,841-13,874.

Smith, W. L. and C. M. R. Platt, 1978: Intercomparison of radiosonde, ground-based laser, and satellite-deduced cloud heights. *J. Appl. Meteor.*, **17**, 1796-1802.

Smith, E. A., and L. Shi, 1992: Surface forcing of the infrared cooling profile over the Tibetan plateau. Part I: Influence of relative longwave radiative heating at high altitude. *J. Atmos. Sci.*, **49**, 805-822.

Stubenrauch, C. J., W. B. Rossow, F. Chéruy, A. Chédin, and N. A. Scott, 1999: Clouds as seen by satellite sounders (3I) and imagers (ISCCP). Part I: Evaluation of cloud parameters. *J. Climate*, **12**, 2189-2213.

Teixeira, J., 1999: The impact of increased boundary layer resolution on the ECMWF forecast system. *ECMWF Technical Memorandum*, **268**, 55 pp. [available from ECMWF, Shinfield Park, Reading, Berks. RG2 9AX, UK]

Ulaby, F. T., R. K. Moore, A. K. Fung, 1981: Microwave remote sensing: active and passive. Volume I. Artech House, 456 pp.

Waliser and Gautier, 1993: A satellite-derived climatology of the ITCZ. *J. Climate*, **6**, 2162-2174.

Washington, W.M. and D.L. Williamson, 1977 : A description of the NCAR GCM's in General circulation models of the atmosphere. Method in Computational Physics, J. Chang. Ed., 17, Academic Press, 11100-17002.

Wylie, D. P., W. P. Menzel, H. M. Woolf, and K. I. Strabala, 1994: Four years of global cirrus cloud statistics using HIRS. *J. Climate*, **7**, 1972-1986.

Wylie, D. P., and W. P. Menzel, 1999: Eight years of high cloud statistics using HIRS. *J. Climate*, **12**, 170-184.